

Carbon-Fiber-Reinforced Concrete as an Intrinsically Smart Concrete for Damage Assessment during Dynamic Loading

Pu-Woei Chen and D. D. L. Chung

Composite Materials Research Laboratory, State University of New York at Buffalo,
Buffalo, New York 14260-4400

Concrete containing short carbon fibers (0.2–0.5 vol%) was found to be an intrinsically smart concrete that can sense elastic and inelastic deformation, as well as fracture. The signal provided is the change in electrical resistance, which is reversible for elastic deformation and irreversible for inelastic deformation and fracture. The presence of electrically conducting short fibers is necessary for the concrete to sense elastic or inelastic deformation, but the sensing of fracture does not require fibers. The fibers serve to bridge the cracks and provide a conduction path. The resistance increase is due to conducting fiber pullout in the elastic regime, conducting fiber breakage in the inelastic regime, and crack propagation at fracture.

I. Introduction

SMART structures capable of damage assessment in real time are important, due to the need to maintain the functions of critical civil infrastructure systems. The sensing provides an electrical, optical, or acoustic response to damage in real time during dynamic loading. Requirements of the sensor include (1) low cost for both materials and implementation, (2) durability and reliability, (3) measurement repeatability and stability, (4) ability to provide quantitative signals with high sensitivity and resolution, (5) ability to provide spatial resolution, (6) fast response, (7) sensitivity to a wide dynamic range of strain, covering both the elastic and inelastic regimes of deformation, (8) not weakening the structure, (9) not requiring expensive peripheral equipment, and (10) applicability to both old and new structures.

Requirement No. 7 above refers to the ability to detect and distinguish between inelastic deformation (which corresponds to permanent damage) and elastic deformation. This ability is valuable for monitoring damage occurrence during dynamic loading, as it provides monitoring of the dynamic loading in its complete range, covering both the elastic and inelastic regimes. Thus, it allows determination of exactly in which part of which loading cycle damage occurs and does not require the load cycling to be periodic in time. No. 5 above refers to the ability to provide a measure of the degree and location of damage. This measure can be in terms of the inelastic strain, as strain in the inelastic regime is associated with damage. The greater the inelastic strain, the greater is the damage. Due to the ability described in No. 7, the response due to the inelastic strain can be distinguished from that due to the elastic strain. Thus, the inelastic strain (or degree of damage) can be monitored in real time during dynamic loading.

A new sensor technology,¹ in which concrete itself is the sensor, satisfies all of the requirements listed above. Moreover, the intrinsically smart concrete exhibits high flexural strength

and toughness, and low drying shrinkage.² In this paper, the sensing ability and its origin are described in relation to the sensing of elastic deformation, inelastic deformation, and fracture. In contrast to techniques such as acoustic emission, which cannot sense elastic deformation, this new sensor technology allows the sensing of elastic deformation, in addition to inelastic deformation and fracture. The signal provided is the change in the electrical resistance. Reversible strain is associated with reversible resistance change; irreversible strain is associated with irreversible resistance change; fracture is associated with irreversible and particularly large resistance change. The origin of the signal associated with fracture is crack propagation, which increases the resistance due to the high resistivity of the cracks. The origin of the signal associated with irreversible strain is conducting fiber breakage; the origin of the signal associated with reversible strain is conducting fiber pullout. The detection of fracture does not require fibers in the concrete, whereas the detection of irreversible and reversible strains requires the presence of short and electrically conducting fibers in the concrete.

II. Experimental Procedure

The fibers were unsized carbon fibers based on isotropic pitch and of diameter 10 μm , nominal length 5 mm, and electrical resistivity $3 \times 10^{-3} \Omega \cdot \text{cm}$. Their amount was 0.5% by weight of cement. The aggregate was natural sand. The mortars studied were (i) plain mortar, (ii) mortar with latex, (iii) mortar with methylcellulose, and (iv) mortar with methylcellulose and silica fume. Latex, methylcellulose and silica fume were added to disperse the fibers, but they were used whether fibers were present or not in order to obtain the effect of the fibers alone.

The water reducing agent was TAMOL SN (Rohm and Haas), which contained 93%–96% sodium salt of a condensed naphthalenesulfonic acid. The slump of carbon-fiber-reinforced cement tends to decrease with increasing carbon fiber content, so we used a water-reducing agent to maintain a flow of 150 ± 50 mm. The latex was styrene butadiene in the amount of 20% of the weight of the cement. The antifoam (Dow Corning 2410) used with the latex was in the amount of 0.5% by weight of latex. Methylcellulose in the amount of 0.4% of the cement weight was used; the defoamer (Colloids 1010) used with it was in the amount of 0.13 vol%.

For the case of mortar containing latex, latex, antifoam and fibers first were mixed by hand for about 1 min. Then this mixture, cement, sand, water, and water-reducing agent were mixed in a Hobart mixer for 5 min. For the case of mortar containing methylcellulose, methylcellulose was dissolved in water. After that, the defoamer and then the fibers were added and stirred by hand for 2 min. Then this mixture, cement, sand, water, and water-reducing agent (and silica fume, if applicable) were mixed in the Hobart mixer for 5 min. For the case of concrete, only the formulation involving methylcellulose and silica fume² was used. After pouring the mix into oiled molds, a vibrator was used to decrease the amount of air bubbles. The specimens were demolded after 1 d and then cured in air (10% rh) for 7 d.

S. M. Wiederhorn—contributing editor

Simultaneous to mechanical testing, resistance measurements were made at a DC current from 0.1 to 4 A. For each test, six specimens of each type were used. For compressive testing according to ASTM C109-80, mortar specimens were prepared by using a $2 \times 2 \times 2$ in. ($5.1 \times 5.1 \times 5.1$ cm) mold. For compressive testing according to ASTM C39-83b, concrete specimens were prepared using a 102 mm (4 in.) diameter \times 203 mm (8 in.) length mold. Dog-bone shaped specimens were used for tensile testing. They were prepared by using molds of the same shape and size. The displacement rate was 1.27 mm/min. During compressive or tensile loading up to fracture, the strain was measured by the crosshead displacement in compressive testing or by a strain gage in tensile testing, while the fractional change in electrical resistance along the stress axis was measured using the four-probe method. The electrical contacts were made by silver paint. Although the spacing between the contacts increased upon tensile deformation and decreased upon compressive deformation, the increase was so small that the measured resistance remained essentially proportional to the resistivity. Testing was performed either in one cycle up to the breaking stress or in multiple cycles upon loading up to a fraction ($1/3$ under compression and $\sim 1/2$ under tension) of the breaking stress.

III. Results

Table I summarizes the results of simultaneous compressive/tensile testing and resistivity measurement along the stress axis. The electrical probing gave the resistance R between the two voltage probes (a distance d apart) in the four-probe setup. Table I gives the fractional change in R at fracture, i.e., $\Delta R/R_0$, where R_0 is the original resistance. For compressive testing, $d = 1$ cm and 4 in. for mortars and concretes, respectively; for tensile testing, $d = 4$ cm (for mortars only). In both compression and tension, $\Delta R/R_0$ is positive, because flaws are generated. $\Delta R/R_0$ at fracture is larger under compression than tension. This is due to the higher ductility under compression. Without fibers, $\Delta R/R_0$ varies randomly with strain/stress up to fracture, at which $\Delta R/R_0$ abruptly increases. $\Delta R/R_0$ did not vary with the fiber content (if nonzero), though the original resistivity decreased much with increasing fiber content.

Under cyclic compressive/tensile loading, without fibers, no smart behavior was observed. With fibers, under cyclic compressive loading within the regime where the strain was essentially fully reversible (Fig. 1), the smart behavior was observed as (i) irreversibly increasing $\Delta R/R_0$ during the first loading, (ii) reversibly increasing $\Delta R/R_0$ during unloading in any cycle, and (iii) reversibly decreasing $\Delta R/R_0$ during the second and subsequent loadings. The irreversibly increasing $\Delta R/R_0$ during the first loading (which involved no irreversible strain) is attributed to the irreversible increase in the contact electrical resistivity at the fiber/matrix interface due to the weakening of that

Table I. Results of Simultaneous Compressive/Tensile Testing and Electrical Resistivity Measurement along the Stress Axis

Mortar*	Vol% fibers	Compressive			Tensile		
		Strength (MPa)	Ductility (%)	$\Delta R/R_0$ at fracture	Strength (MPa)	Ductility (%)	$\Delta R/R_0$ at fracture
Plain	0	35.6	0.16	69.5	0.88	0.004	0.88
L	0	38.6	0.24	30	3.03	0.0352	0.6
L	0.37	37.8	0.17	4.1			
L	0.53				3.15	0.0413	0.053
M	0	34.5	0.17	3.4	1.37	0.0209	0.18
M	0.24	33.6	0.15	10.42			
M	0.53				1.95	0.0192	0.034
M+SF	0	42.7	0.16	9.7	0.83	0.088	0.037
M+SF	0.24	41.0	0.19	21.14			
M+SF	0.53				1.88	0.0173	0.051

*L = latex, M = methylcellulose, SF = silica fume, F = fibers.

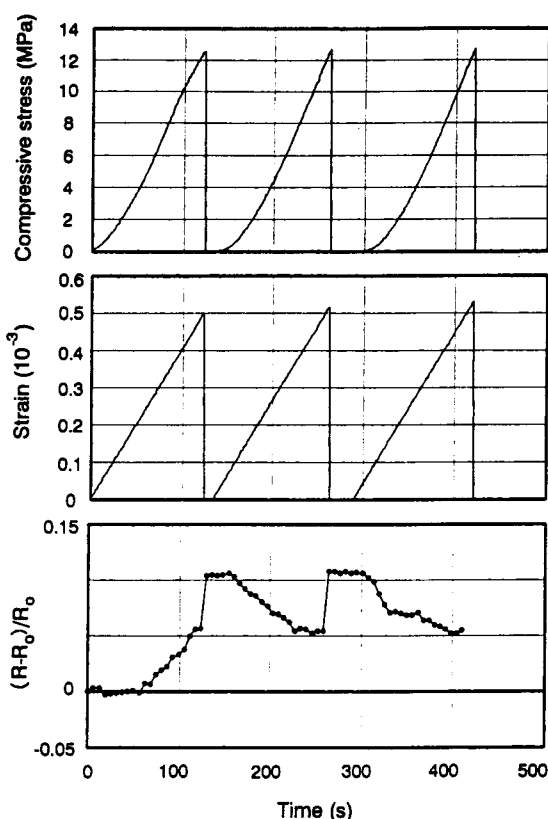


Fig. 1. Plots vs time of $\Delta R/R_0$, compressive strain and compressive stress obtained during cyclic compressive testing for mortar containing methylcellulose and 0.24 vol% fibers.

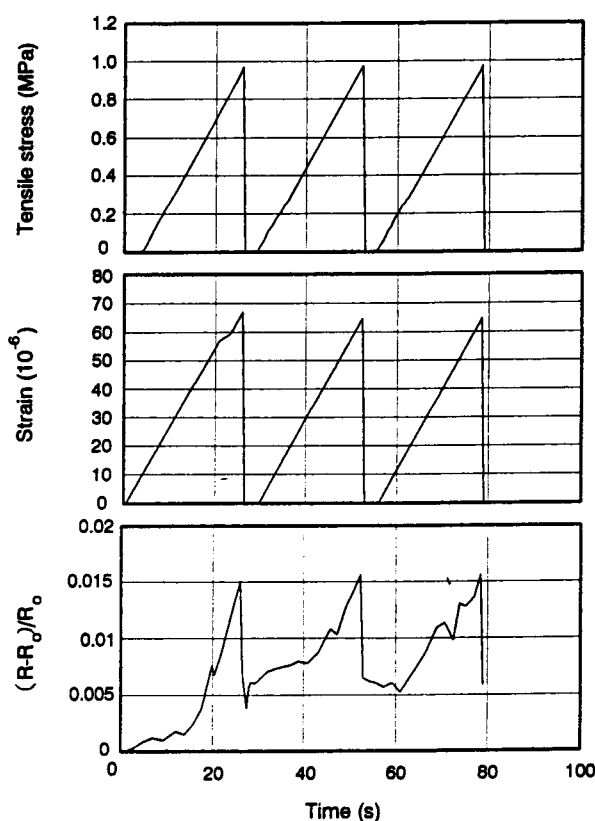


Fig. 2. Plots vs time of $\Delta R/R_0$, tensile strain and tensile stress obtained during cyclic tensile testing for mortar containing methylcellulose and 0.53 vol% fibers.

interface. The reversibly increasing $\Delta R/R_0$ during unloading in any cycle is attributed to crack opening (i.e., increase in the length or height of a crack), which was hindered under compressive loading. The reversibly decreasing $\Delta R/R_0$ during the second and subsequent loadings is attributed to crack closure (i.e., decrease in the length or height of a crack) under compressive loading. The reversibility of the crack opening is attributed to the fiber bridging across the crack. The occurrence of fiber pullout requires a relatively weak fiber/matrix interface, which is provided by the interface weakening associated with the irreversible increase in $\Delta R/R_0$ prior to the fiber pullout or crack opening. Under cyclic tensile loading within the regime where the strain was fully reversible (Fig. 2), the smart behavior was observed as (i) irreversibly increasing $\Delta R/R_0$ during the initial portion of the first loading, (ii) reversibly increasing $\Delta R/R_0$ during the latter portion of the first loading and during any subsequent loading, and (iii) reversibly decreasing $\Delta R/R_0$ during unloading in any cycle. The increase in $\Delta R/R_0$ during loading is attributed to crack opening, whereas the decrease in $\Delta R/R_0$ during unloading is attributed to crack closure. That the initial portion of the first loading exhibited irreversibly increasing $\Delta R/R_0$, whereas the latter portion was reversible is because the irreversible part is due to the fiber/matrix interface weakening, whereas the reversible part is due to crack opening. Consistent results were obtained on concretes, though $\Delta R/R_0$ was smaller for concrete than mortar.

The fractions $(\Delta R/R_0)_{\text{reversible}}/(\Delta R/R_0)_{\text{fracture}}$ and $(\Delta R/R_0)_{\text{irreversible}}/(\Delta R/R_0)_{\text{fracture}}$ vary with the stress amplitude in cyclic loading. In Table II, the stress amplitude is expressed as the maximum stress divided by the fracture stress. The fractions listed are for compression of mortars containing latex and 0.37 vol% fibers.

Table II. Effect of Stress Amplitude in Cyclic Compressive Loading on the Reversible and Irreversible Parts of $(\Delta R/R_0)/(\Delta R/R_0)_{\text{fracture}}$ and the Reversible and Irreversible Parts of Strain/Strain_{fracture} for Mortar Containing Latex and 0.37 vol% Carbon Fibers

Max. stress Fracture stress	$(\Delta R/R_0)/(\Delta R/R_0)_{\text{fracture}}$		Strain/strain _{fracture}	
	Reversible	Irreversible	Reversible	Irreversible
0.75	0.039	0.244	0.29	0.44
0.65	0.037	0.102	0.29	0.33
0.50	0.032	0.115	0.38	0.12
0.40	0.0073	0.068	0.33	0.09
0.33	0.0034	0.0015	0.32	0.01
0.25	0.0025	0.0013	0.29	0.00
0.20	0.0027	0.0017	0.27	0.00

The irreversible strain increases monotonically with the stress amplitude, but the reversible strain does not vary with the stress amplitude. Table II shows good correlation between the irreversible strain and the irreversible part of $\Delta R/R_0$.

The effect of the fiber addition on the crack height was examined after compression to 70% of the fracture stress for (a) mortar containing latex but no fibers, and (b) mortar containing latex and 0.37 vol% fibers. These mortars have similar compressive strength (Table I). The crack height was 1 μm in (b) and 100 μm in (a), indicating that the fibers caused crack opening control, which in turn resulted in the smart behavior. Table I shows significant effects of the fiber addition on the tensile and flexural properties.

When the carbon fibers in the latex-containing mortar were replaced by stainless steel fibers (60 μm diameter, 5 mm length, $6 \times 10^{-5} \Omega \cdot \text{cm}$ electrical resistivity, 0.37 vol%), an electrical response was observed under compression, though the plot of $\Delta R/R_0$ vs strain was more noisy than in the carbon fiber case, probably because of the large diameter of the steel fibers. However, when the carbon fibers were replaced by polyethylene fibers (Spectra 900, 38 μm diameter, 5 mm length, 0.37 vol%), no electrical response was observed. Thus, the conducting nature of the fibers is necessary for the electrical response to elastic or inelastic deformation.

IV. Conclusion

Carbon-fiber-reinforced concrete was found to be an intrinsically smart concrete that can sense elastic and inelastic deformation and fracture. The signal provided is the change in electrical resistance, which is reversible for elastic deformation and irreversible for inelastic deformation and fracture. The presence of electrically conducting short fibers is necessary for the concrete to sense elastic or inelastic deformation, though the sensing of fracture does not require fibers. The fibers bridge the cracks and provide a conduction path. They do not need to touch one another. The electrical resistance increase is due to conducting fiber pullout in the elastic regime, conducting fiber breakage in the inelastic regime, and crack propagation at fracture. The fractional change in resistance at fracture is higher under compression than under tension, due to the higher ductility under compression.

References

- ¹P.-W. Chen and D. D. L. Chung, "Carbon Fiber Reinforced Concrete for Smart Structures Capable of Non-destructive Flaw Detection," *Smart Mater. Struct.*, **2**, 22-30 (1993).
- ²P.-W. Chen and D. D. L. Chung, "Concrete Reinforced with up to 0.2 vol.% of Short Carbon Fibres," *Composites (Guildford, U.K.)*, **24**, 33-52 (1993). □